Noname manuscript No.
(will be inserted by the editor)

On the parameter choice in grad-div stabilization for incompressible flow problems

Eleanor W. Jenkins · Volker John · Alexander Linke · Leo G. Rebholz

Abstract Grad-div stabilization has been proved to be a very useful tool in discretizations of incompressible flow problems. Standard error analysis for inf-sup stable conforming pairs of finite element spaces predicts that the stabilization parameter should be optimally chosen to be $\mathcal{O}(1)$. This paper revisits this choice for the Stokes equations on the basis of minimizing the $H^1(\Omega)$ error of the velocity and the $L^2(\Omega)$ error of the pressure. It turns out, by applying a refined error analysis, that the optimal parameter choice is more subtle than known so far in the literature. It depends on the used norm, the solution, the family of finite element spaces, and the type of mesh. Depending on the situation, the optimal stabilization parameter might range from being very small to very large. The analytic results are supported by numerical examples.

Keywords Incompressible Navier-Stokes equations · Mixed finite elements · Grad-div stabilization · Error estimates · Parameter choice

Mathematics Subject Classification (2000) 35Q30 · 76M10 · 65L60

1 Introduction

This paper investigates the choice of the parameter for grad-div stabilization in mixed finite element methods for the Stokes equations, which are given by

$$-\nu\Delta\mathbf{u} + \nabla p = \mathbf{f}, \quad \nabla\cdot\mathbf{u} = 0 \quad \text{in } \Omega.$$

Grad-div stabilization results from adding $\mathbf{0} = -\gamma\nabla(\nabla\cdot\mathbf{u})$ to the continuous Stokes equations, which yields the term $\gamma(\nabla\cdot\mathbf{u}_h, \nabla\cdot\mathbf{v}_h)$ in the finite element formulation. Since $\nabla\cdot\mathbf{u}_h \neq 0$ for most common finite element methods for the Stokes equations, due to the only discrete enforcement of the divergence-free condition, this additional term is non-zero and acts to penalize a lack of mass conservation. It is well known that the use of this type of consistent stabilization can improve solution accuracy [17], conditioning of discrete systems [9], convergence of iterative solvers [5,19], and even solution accuracy for related problems such as the Navier–Stokes equations, Boussinesq equations, and others [7,14,8,13,15,20,11].

Due to the proven usefulness of grad-div stabilization, there is a natural interest to deepen its understanding, and in particular to study how to choose the stabilization parameter γ optimally. Theoretical

A. Linke supported by the DFG Research Center Matheon, project D27.

L. G. Rebholz partially supported by NSF grant DMS1112593.

E. W. Jenkins
Department of Mathematical Sciences, Clemson University, U.S.A., E-mail: lea@clemson.edu

V. John
Weierstrass Institute for Applied Analysis and Stochastics, Mohrenstr. 39, 10117 Berlin, Germany and Free University of Berlin, Department of Mathematics and Computer Science, Arnimallee 6, 14195 Berlin, Germany,
E-mail: volker.john@wias-berlin.de

A. Linke
Free University of Berlin, Department of Mathematics and Computer Science, Arnimallee 6, 14195 Berlin, Germany,
E-mail: alexander.linke@wias-berlin.de

L. G. Rebholz
Department of Mathematical Sciences, Clemson University, U.S.A., E-mail: rebholz@clemson.edu

analysis and numerical simulations, e.g., from [16,17,19,3], suggest that $\gamma = \mathcal{O}(1)$ is an appropriate choice in the context of inf-sup stable conforming finite element spaces, and this seems to be widely accepted in the community. However, it was recently shown in [8] that in certain situations, an optimal γ can actually be much larger than $\mathcal{O}(1)$. There, the authors showed analytically and with numerical studies that for solutions with very large or complicated pressures, e.g., caused by irrotational forcing, one gets very good results with $\gamma = 10^4$ and bad results with $\gamma = 1$ or 10.

The goals of the present paper are to demonstrate for the simplest model problem, the Stokes equations, that

- the choice of the grad-div stabilization parameter from the analytic point of view is more involved than it can be found so far in the literature, if the error in the $H^1(\Omega)$ norm of the velocity is of primary interest,
- an enormous increase in accuracy can be achieved sometimes by using a parameter that is predicted by the analysis presented in this paper, instead of a standard $\mathcal{O}(1)$ parameter.

The Stokes equations are considered, i.e. instead of Navier-Stokes, in order to concentrate on the main statement of this paper, the more subtle choice of the stabilization parameter than it is known so far, without introducing technical difficulties that arise, e.g., from the consideration of nonlinear problems. In particular, it will be shown first that for minimizing the $H^1(\Omega)$ velocity error the optimal parameter choice depends critically on the magnitude of the pressure relative to the velocity in appropriate norms. A statement of this form can be also found in [16,10], but the possibly large stabilization parameter is not investigated further. Secondly, it depends on whether the pointwise divergence-free subspace of the finite element velocity space has some optimal approximation properties, which seems to be a new observation. These properties are closely related with the specific choice of the finite element space, i.e., with the family of finite elements and with the mesh. These results will be derived by performing a finite element error analysis for the $H^1(\Omega)$ velocity error, considering it as a function of γ, and then minimizing it. It will be also demonstrated that one obtains different optimal stabilization parameters if one considers the $L^2(\Omega)$ error of the pressure.

It turns out, depending on the specific situation, that the optimal stabilization parameter might be of very different size, e.g., it might depend on the mesh width h. We like to remark that although the theory consists essentially in refining a standard analysis, it is able to predict phenomena seemingly unobserved before. However, it does not lead to a formula for choosing the grad-div stabilization parameter that can be used instantly in practice since the formulas involve usually unknown constants and norms of derivatives of the velocity and pressure solution of the continuous Stokes equations. Instead, the theory provides a qualitative understanding for the practitioner, how the discretization method and the mesh influence the choice of a good stabilization parameter.

The paper starts by introducing the continuous and the discrete Stokes equations as well as the space of divergence-free and discretely divergence-free functions in Section 2. Section 3 presents the finite element error analysis that leads to good parameter choices for minimizing different errors and for different approximation properties of the pointwise divergence-free subspace. Numerical studies, presented in Section 4, support the analytic results. In particular, it is shown that, depending on the example, the finite element space, and the mesh, the optimal parameter might be vary from $\mathcal{O}(h^2)$ to $\mathcal{O}(10^3)$. Section 5 summarizes the results and further steps are discussed that are necessary for the application of the theory to more difficult problems than considered in this paper. Throughout the paper, standard notations are used for usual function spaces, norms, and inner products.

2 The setup of the problem and its finite element discretization

This paper considers the Stokes equations with homogeneous Dirichlet boundary conditions: find $(\mathbf{u}, p) \in H_0^1(\Omega)^d \times L_0^2(\Omega)$ in a Lipschitz domain with polyhedral boundary $\Omega \subset \mathbb{R}^d$, $d \in \{2,3\}$, such that, for all $(\mathbf{v}, q) \in H_0^1(\Omega)^d \times L_0^2(\Omega)$ it holds

$$\begin{aligned} \nu(\nabla \mathbf{u}, \nabla \mathbf{v}) - (\nabla \cdot \mathbf{v}, p) &= (\mathbf{f}, \mathbf{v}), \\ (\nabla \cdot \mathbf{u}, q) &= 0. \end{aligned} \tag{2.1}$$

For the finite element discretization, we choose pairs of conforming finite element spaces $V_h \subset H_0^1(\Omega)^d$ and $Q_h \subset L_0^2(\Omega)$ that satisfy the inf-sup stability condition (BB condition, LBB condition), see, e.g. [4,12],

$$\inf_{q_h \in Q_h} \sup_{\mathbf{v}_h \in V_h} \frac{(\nabla \cdot \mathbf{v}_h, q_h)}{\|\nabla \mathbf{v}_h\|_0 \, \|q_h\|_0} \geq \beta > 0. \tag{2.2}$$

In addition, the discrete bilinear form is extended with a grad-div stabilization in order to mitigate problems with poor mass conservation. Then, the stabilized finite element discretization reads: For fixed $\gamma \geq 0$, find $(\mathbf{u}_h, p_h) \in V_h \times Q_h$ such that for all $(\mathbf{v}_h, q_h) \in V_h \times Q_h$

$$\begin{aligned} \nu(\nabla \mathbf{u}_h, \nabla \mathbf{v}_h) + \gamma(\nabla \cdot \mathbf{u}_h, \nabla \cdot \mathbf{v}_h) - (\nabla \cdot \mathbf{v}_h, p_h) &= (\mathbf{f}, \mathbf{v}_h), \\ (\nabla \cdot \mathbf{u}_h, q_h) &= 0. \end{aligned} \tag{2.3}$$

We introduce now the spaces of weakly differentiable divergence-free functions, and discretely divergence-free functions

$$\begin{aligned} V_0 &= \{\mathbf{v} \in H_0^1(\Omega)^d \ : \ \nabla \cdot \mathbf{v} = 0\}, \\ V_{0,h} &= \{\mathbf{v}_h \in V_h \ : \ (\nabla \cdot \mathbf{v}_h, q_h) = 0 \ \text{ for all } q_h \in Q_h\}. \end{aligned}$$

In general, $V_{0,h} \not\subset V_0$, i.e., discretely divergence-free functions need not to be divergence-free. Note that there are only few pairs of finite element spaces that satisfy $V_{0,h} \subset V_0$. The space of divergence-free and discretely divergence-free functions

$$V_{00,h} := V_{0,h} \cap V_0$$

will become important for an appropriate choice of the stabilization parameter γ.

Definition 1 (Optimal approximation properties of the divergence-free subspace) Consider a sequence of quasi-uniform meshes with characteristic mesh size h and the corresponding spaces $V_{00,h}$. If for all $\mathbf{v} \in V_0 \cap H^{k+1}(\Omega)^d$ there exists a sequence of $\mathbf{v}_h \in V_{00,h}$ with

$$\|\nabla \mathbf{v} - \nabla \mathbf{v}_h\|_0 \leq C_{V_{00,h}} h^k |\mathbf{v}|_{k+1},$$

with $C_{V_{00,h}}$ independent of h, then the sequence of spaces $V_{00,h}$ is said to possess optimal approximation properties (w.r.t. the space V_0).

3 On choices of the grad-div parameter that are based on error estimates

The goal of the following analysis consists of finding good values for the stabilization parameter γ. It will be shown that the standard parameter choice $\gamma \sim \mathcal{O}(1)$, presented, e.g., in [17,19], is not always adequate, and that it can even be far from being optimal. This standard choice is justified in a paradigmatic way in the excellent article [17] by deriving an optimal a-priori estimate for (2.3). We like to emphasize that the estimate of the optimal stabilization parameter in [17] is based on the norm $(\nu \|\nabla \mathbf{u}\|_0^2 + \gamma \|\nabla \cdot \mathbf{u}\|^2 + \|p\|_0^2)^{\frac{1}{2}}$, which is called there the 'natural norm'. In contrast, we will search first for optimality with respect to the velocity norm $\|\nabla \mathbf{u}\|_0$, since one is often mainly interested in the control of this error. Following this analysis, it will be demonstrated that the asymptotic optimal choice of γ which is based on the consideration of the error in the $L^2(\Omega)$ pressure norm leads to different values as were derived for the error in the velocity norm. The choice of a different norm with respect to the derivations in [17,19], as well as the refined analysis, seem to explain the different results.

3.1 Appropriate choices of the grad-div parameter based on a velocity error estimate

We consider now the $H^1(\Omega)$ velocity error of the discrete Stokes system with grad-div stabilization (2.3) and use the resulting error estimate to find a good choice for γ.

Theorem 1 *For a given $\mathbf{f} \in H^{-1}(\Omega)^d$, let $(\mathbf{u}, p)$ be the solution to (2.1), and let $(\mathbf{u}_h, p_h)$ be the solution to (2.3). Then, the error in the $L^2(\Omega)$ norm of the gradient of the velocity is bounded by*

$$\|\nabla(\mathbf{u} - \mathbf{u}_h)\|_0^2 \leq \inf_{\mathbf{w}_h \in V_{0,h}} \left(4\|\nabla(\mathbf{u} - \mathbf{w}_h)\|_0^2 + 2\frac{\gamma}{\nu} \|\nabla \cdot \mathbf{w}_h\|_0^2 \right) + \frac{2}{\gamma\nu} \inf_{q_h \in Q_h} \|p - q_h\|_0^2. \tag{3.1}$$

Proof Write $\mathbf{u}-\mathbf{u}_h = (\mathbf{u}-\mathbf{w}_h)+(\mathbf{w}_h-\mathbf{u}_h) =: \boldsymbol{\eta}+\boldsymbol{\psi}_h$, where $\mathbf{w}_h \in V_{0,h}$ is arbitrary. First, by the triangle inequality and Young's inequality, one obtains

$$\|\nabla\mathbf{u}-\nabla\mathbf{u}_h\|_0^2 \leq 2\,\|\nabla\boldsymbol{\eta}\|_0^2 + 2\,\|\nabla\boldsymbol{\psi}_h\|_0^2. \tag{3.2}$$

For any $\mathbf{v}_h \in V_{0,h}$, one concludes by subtracting (2.1) and (2.3) that

$$\nu(\nabla\boldsymbol{\psi}_h,\nabla\mathbf{v}_h)+\gamma(\nabla\cdot\boldsymbol{\psi}_h,\nabla\cdot\mathbf{v}_h) = -\nu(\nabla\boldsymbol{\eta},\nabla\mathbf{v}_h)-\gamma(\nabla\cdot\boldsymbol{\eta},\nabla\cdot\mathbf{v}_h)+(\nabla\cdot\mathbf{v}_h,p).$$

Choosing $\mathbf{v}_h = \boldsymbol{\psi}_h$, and using that $(\nabla\cdot\boldsymbol{\psi}_h,q_h)=0$ for any $q_h\in Q_h$, the error equation becomes, for any $q_h\in Q_h$,

$$\nu\|\nabla\boldsymbol{\psi}_h\|_0^2+\gamma\|\nabla\cdot\boldsymbol{\psi}_h\|_0^2 = -\nu(\nabla\boldsymbol{\eta},\nabla\boldsymbol{\psi}_h)-\gamma(\nabla\cdot\boldsymbol{\eta},\nabla\cdot\boldsymbol{\psi}_h)+(\nabla\cdot\boldsymbol{\psi}_h,p-q_h).$$

After applying the Cauchy-Schwarz and Young's inequality on the right hand side, one gets

$$\nu\|\nabla\boldsymbol{\psi}_h\|_0^2+\gamma\|\nabla\cdot\boldsymbol{\psi}_h\|_0^2 \leq \nu\|\nabla\boldsymbol{\eta}\|_0^2+\gamma\|\nabla\cdot\boldsymbol{\eta}\|_0^2+2\|p-q_h\|_0\|\nabla\cdot\boldsymbol{\psi}_h\|_0. \tag{3.3}$$

The last term on the right hand side can be majorized by

$$2\|p-q_h\|_0\|\nabla\cdot\boldsymbol{\psi}_h\|_0 \leq \gamma^{-1}\|p-q_h\|_0^2+\gamma\|\nabla\cdot\boldsymbol{\psi}_h\|_0^2, \tag{3.4}$$

which leads to

$$\|\nabla\boldsymbol{\psi}_h\|_0^2 \leq \|\nabla\boldsymbol{\eta}\|_0^2+\frac{\gamma}{\nu}\|\nabla\cdot\boldsymbol{\eta}\|_0^2+\frac{1}{\gamma\nu}\inf_{q_h\in Q_h}\|p-q_h\|_0^2.$$

Finally, (3.2) gives

$$\|\nabla\mathbf{u}-\nabla\mathbf{u}_h\|_0^2 \leq 4\|\nabla\boldsymbol{\eta}\|_0^2+2\frac{\gamma}{\nu}\|\nabla\cdot\boldsymbol{\eta}\|_0^2+\frac{2}{\gamma\nu}\inf_{q_h\in Q_h}\|p-q_h\|_0^2$$

for all $\mathbf{w}_h\in V_{0,h}$, which is just the statement of the theorem.

For studying the consequences of the error bound (3.1) on the choice of γ, we distinguish two different cases. These two cases are characterized by whether or not the pointwise divergence-free subspace of the velocity space has optimal approximation properties.

Corollary 1 (Taylor–Hood elements) *Consider* $(V_h,Q_h) = ((P_k)^d, P_{k-1})$ *on quasi-uniform meshes and assume that the solution* $(\mathbf{u},p)$ *of* (2.1) *lies in* $H^{k+1}(\Omega)^d \times H^k(\Omega)$.

Case 1) In the general case, if $V_{00,h}$ *does not have optimal approximation properties, then the a-priori estimate of Theorem 1 has the form*

$$\|\nabla\mathbf{u}-\nabla\mathbf{u}_h\|_0^2 \leq \left(4+\frac{2\gamma}{\nu}\right)C_{V_{0,h}}^2h^{2k}|\mathbf{u}|_{k+1}^2+\frac{2C_{Q_h}^2}{\gamma\nu}h^{2k}|p|_k^2. \tag{3.5}$$

Case 2) If $V_{00,h}$ *has optimal approximation properties, one obtains the a-priori error estimate*

$$\|\nabla\mathbf{u}-\nabla\mathbf{u}_h\|_0^2 \leq \min\left\{\left(4+\frac{2\gamma}{\nu}\right)C_{V_{0,h}}^2, 4C_{V_{00,h}}^2\right\}h^{2k}|\mathbf{u}|_{k+1}^2+\frac{2C_{Q_h}^2}{\gamma\nu}h^{2k}|p|_k^2. \tag{3.6}$$

The constants $C_{Q_h}, C_{V_{00,h}}, C_{V_{0,h}}$ *are constants coming from interpolation estimates, where* $C_{V_{00,h}}$ *and* $C_{V_{0,h}}$ *depend on* β^{-1}.

Proof For the first case, one can only use that $\|\nabla\cdot\mathbf{w}_h\| = \|\nabla\cdot(\mathbf{u}-\mathbf{w}_h)\| \leq \|\nabla(\mathbf{u}-\mathbf{w}_h)\|$ holds in this setting. Then, one applies standard approximation theory to prove (3.5).

For the second case, if the space $V_{00,h}$ has optimal approximation properties, one gets an additional estimate. Here, one can choose $\mathbf{w}_h\in V_{00,h}$ in (3.1). Hence, the velocity error term can be bounded also by

$$\inf_{\mathbf{w}_h\in V_{0,h}}\left(4\|\nabla(\mathbf{u}-\mathbf{w}_h)\|_0^2+2\frac{\gamma}{\nu}\|\nabla\cdot\mathbf{w}_h\|_0^2\right) \leq 4C_{V_{00,h}}^2h^{2k}|\mathbf{u}|_{k+1}^2,$$

since $2\frac{\gamma}{\nu}\|\nabla\cdot\mathbf{w}_h\|_0^2$ vanishes. Combining both results gives (3.6). Typically, $C_{V_{00,h}}$ is significantly larger than $C_{V_{0,h}}$.

Remark 1 (Taylor–Hood elements) The two different cases from Corollary 1 will be discussed now in more detail.

Case 1) If $V_{00,h}$ does not have optimal approximation properties, one can regard the right hand side of (3.5) as a function dependent on γ. This function has a minimum which can be determined by elementary calculus:

$$\gamma_{\text{opt}} \approx \frac{C_{Q_h}}{C_{V_{0,h}}} \frac{|p|_k}{|\mathbf{u}|_{k+1}}. \tag{3.7}$$

We emphasize that γ_{opt} may be quite large, whenever the velocity norm is small compared with the pressure norm, and that this situation can happen in practice, e.g., in coupled flow problems like Rayleigh–Bénard convection, see Section 4.

Case 2) If $V_{00,h}$ has optimal approximation properties, the right hand side of estimate (3.6) is not as easy to analyze. The numerical results in Figure 2 show, depending on the complexity of the pressure, there may or there may be not an optimal γ, since for $|p|_k \gg |\mathbf{u}|_{k+1}$ one has $\gamma_{\text{opt}} = \infty$, which is not feasible in practice (but is equivalent to using $((P_2)^2, P_1^{\text{disc}})$ Scott–Vogelius elements [6]). Therefore, giving up the idea of finding the optimal γ, we only want to find a good γ, which should not be ∞. We used as criterion for the choice of γ that the contribution of the pressure error equals the maximum possible contribution of the velocity error $4C^2_{V_{00,h}} h^{2k} |\mathbf{u}|^2_{k+1}$, which is already asymptotically optimal. This criterion leads to

$$\gamma_{\text{good}} \approx \frac{1}{2\nu} \left(\frac{C_{Q_h}}{C_{V_{00,h}}} \frac{|p|_k}{|\mathbf{u}|_{k+1}} \right)^2. \tag{3.8}$$

The numerical studies in Section 4 will show that this consideration delivers good results. It is interesting that only in the second case γ_{good} is ν-dependent, which can be observed in the numerical examples as well. For both cases, one does not observe a dependence on the mesh width h.

The corollary and remark above are specific to Taylor–Hood elements, but the same techniques can be applied to any conforming inf-sup stable finite element pair used for computing solutions of (2.3). Naturally, results for optimal stabilization parameter γ will vary. In the numerical experiments in Section 4, the theory will be tested on both the Taylor–Hood element and the Mini element.

3.2 Appropriate choices of the grad-div parameter based on a pressure error estimate

We consider now the effect of grad-div stabilization on the $L^2(\Omega)$ pressure error, and how the optimal parameter scales with the problem data.

Theorem 2 *For a given $\mathbf{f} \in H^{-1}(\Omega)^d$, let $(\mathbf{u}, p)$ be the solution to (2.1), let $(\mathbf{u}_h, p_h)$ be the solution to (2.3), and assume for the inf-sup constant $0 < \beta \leq \mathcal{O}(1)$. Then the pressure error is bounded by*

$$\begin{aligned} \|p - p_h\|_0 \leq C(\beta^{-1}) \Bigg\{ & \left(1 + \left(\frac{\nu}{\gamma}\right)^{1/2}\right) \inf_{q_h \in Q_h} \|p - q_h\|_0 \\ & + \inf_{\mathbf{w}_h \in V_{0,h}} \left(\left(\nu + (\nu\gamma)^{1/2}\right) \|\nabla(\mathbf{u} - \mathbf{w}_h)\|_0 + \left((\nu\gamma)^{1/2} + \gamma\right) \|\nabla \cdot \mathbf{w}_h\|_0 \right) \Bigg\}. \end{aligned} \tag{3.9}$$

Proof Equations (2.1) and (2.3) provide us $\forall \mathbf{v}_h \in V_h$ with

$$(p - p_h, \nabla \cdot \mathbf{v}_h) = \nu(\nabla(\mathbf{u} - \mathbf{u}_h), \nabla \mathbf{v}_h) + \gamma(\nabla \cdot (\mathbf{u} - \mathbf{u}_h), \nabla \cdot \mathbf{v}_h).$$

Writing $p - p_h = (p - q_h) + (q_h - p_h)$ for arbitrary $q_h \in Q_h$, and dividing both sides by $\|\nabla \mathbf{v}_h\|$ and reducing gives

$$\begin{aligned} \frac{(q_h - p_h, \nabla \cdot \mathbf{v}_h)}{\|\nabla \mathbf{v}_h\|_0} &= \nu \frac{(\nabla(\mathbf{u} - \mathbf{u}_h), \nabla \mathbf{v}_h)}{\|\nabla \mathbf{v}_h\|_0} + \gamma \frac{(\nabla \cdot (\mathbf{u} - \mathbf{u}_h), \nabla \cdot \mathbf{v}_h)}{\|\nabla \mathbf{v}_h\|_0} - \frac{(\nabla \cdot \mathbf{v}_h, p - q_h)}{\|\nabla \mathbf{v}_h\|_0} \\ &\leq \nu \|\nabla(\mathbf{u} - \mathbf{u}_h)\|_0 + \gamma \|\nabla \cdot (\mathbf{u} - \mathbf{u}_h)\|_0 + \|p - q_h\|_0 . \end{aligned}$$

Next, applying the inf-sup stability (2.2) implies that

$$\beta \|p_h - q_h\|_0 \leq \nu \|\nabla(\mathbf{u} - \mathbf{u}_h)\|_0 + \gamma \|\nabla \cdot (\mathbf{u} - \mathbf{u}_h)\|_0 + \|p - q_h\|_0$$

for any $q_h \in Q_h$. Hence by the triangle equality one obtains

$$\|p - p_h\|_0 \leq \frac{\nu}{\beta} \|\nabla(\mathbf{u} - \mathbf{u}_h)\|_0 + \frac{\gamma}{\beta} \|\nabla \cdot (\mathbf{u} - \mathbf{u}_h)\|_0 + \left(1 + \frac{1}{\beta}\right) \inf_{q_h \in Q_h} \|p - q_h\|_0 . \tag{3.10}$$

From (3.1) it follows immediately that

$$\|\nabla(\mathbf{u} - \mathbf{u}_h)\|_0 \leq \inf_{\mathbf{w}_h \in V_{0,h}} \left(2\|\nabla(\mathbf{u} - \mathbf{w}_h)\|_0 + \left(\frac{2\gamma}{\nu}\right)^{1/2} \|\nabla \cdot \mathbf{w}_h\|_0 \right) + \left(\frac{2}{\gamma\nu}\right)^{1/2} \inf_{q_h \in Q_h} \|p - q_h\|_0. \tag{3.11}$$

Applying to (3.3)

$$2\|p - q_h\|_0 \|\nabla \cdot \boldsymbol{\psi}_h\|_0 \leq 2\gamma^{-1} \|p - q_h\|_0^2 + \frac{\gamma}{2} \|\nabla \cdot \boldsymbol{\psi}_h\|_0^2$$

instead of (3.4), one can derive with the same arguments the estimate

$$\|\nabla \cdot (\mathbf{u} - \mathbf{u}_h)\|_0 \leq \inf_{\mathbf{w}_h \in V_{0,h}} \left(\left(\frac{2\nu}{\gamma}\right)^{1/2} \|\nabla(\mathbf{u} - \mathbf{w}_h)\|_0 + \left(1 + \sqrt{2}\right) \|\nabla \cdot \mathbf{w}_h\|_0 \right) + \frac{2}{\gamma} \inf_{q_h \in Q_h} \|p - q_h\|_0. \tag{3.12}$$

Then from (3.10)–(3.12), one gets

$$\begin{aligned} \|p - p_h\|_0 \leq \beta^{-1} \Bigg\{ & \left(\beta + 1 + 2 + \left(\frac{2\nu}{\gamma}\right)^{1/2} \right) \inf_{q_h \in Q_h} \|p - q_h\|_0 \\ & + \inf_{\mathbf{w}_h \in V_{0,h}} \left(\left(2\nu + (2\nu\gamma)^{1/2}\right) \|\nabla(\mathbf{u} - \mathbf{w}_h)\|_0 + \left((2\nu\gamma)^{1/2} + \left(1 + \sqrt{2}\right)\gamma\right) \|\nabla \cdot \mathbf{w}_h\|_0 \right) \Bigg\}, \end{aligned}$$

and assuming that $\beta \leq \mathcal{O}(1)$ allows this to be reduced to (3.9).

Note that the assumption on β is without loss of generality. If (2.2) holds for some positive β, it holds also for all positive stabilization parameters smaller than β.

The impact of the error bound (3.9) on the choice of the stabilization parameter will be studied in more detail again for the pairs of Taylor–Hood elements.

Corollary 2 (Taylor–Hood elements) *Let the conditions of Corollary 1 hold.*

Case 1) If $V_{00,h}$ does not have optimal approximation properties, one obtains the error estimate

$$\|p - p_h\|_0 \leq C(\beta^{-1}) \left(\left(1 + \left(\frac{\nu}{\gamma}\right)^{1/2}\right) C_{Q_h} h^k |p|_k + \left(\nu + (\nu\gamma)^{1/2} + \gamma\right) C_{V_{0,h}} h^k |\mathbf{u}|_{k+1} \right). \tag{3.13}$$

Case 2) If $V_{00,h}$ has optimal approximation properties, the additional a-priori error estimate becomes

$$\begin{aligned} \|p - p_h\|_0 \leq C(\beta^{-1}) \Bigg(& \left(1 + \left(\frac{\nu}{\gamma}\right)^{1/2}\right) C_{Q_h} h^k |p|_k \\ & + \min\left\{ \left(\nu + (\nu\gamma)^{1/2} + \gamma\right) C_{V_{0,h}}, \left(\nu + (\nu\gamma)^{1/2}\right) C_{V_{00,h}} \right\} h^k |\mathbf{u}|_{k+1} \Bigg). \end{aligned} \tag{3.14}$$

Proof The statements follow with the same arguments as were used in the proof of Corollary 1.

Remark 2 Similar to the velocity case, we want to find good values for γ. However, minimizing the a priori error estimate with respect to γ is more complex than in the velocity case. For instance, the necessary condition for getting the optimal value of γ from (3.13) leads to an equation of the form

$$\frac{\nu}{4} \left(\frac{C_{Q_h} |p|_k}{C_{V_{0,h}} |\mathbf{u}|_{k+1}} - \gamma \right)^2 = \gamma^3. \tag{3.15}$$

Standard calculus gives that there is at least one non-negative value of γ that satisfies (3.15) which is smaller than $(C_{Q_h}|p|_k)/(C_{V_{0,h}}|\mathbf{u}|_{k+1})$. This value is the most left non-negative intersection of the curves on both sides of (3.15). Since the right hand side of (3.13) is a continuous function for $\gamma \in (0, \infty)$ with the limit ∞ at both ends of this interval, the most left local extremum must be a minimum. In the interesting case that ν is small, the curve on the left hand side of (3.15) becomes flat and then there will be exactly

one intersection of both curves, which has to correspond to a minimum and which has to be smaller than $(C_{Q_h}|p|_k)/(C_{V_{0,h}}|\mathbf{u}|_{k+1})$. We could not obtain an analytic expression for this minimum, but a comparison with (3.7) shows already that one gets a different (smaller) optimum than obtained for minimizing the $H^1(\Omega)$ error of the velocity. In the case of small ν, where the lowest powers of ν are of importance, a slight dependence $\gamma_{\text{good}} = \mathcal{O}(\nu^{1/3})$ can be deduced from (3.15).

Considering Case 2 on the same basis like in Remark 1 gives

$$\gamma_{\text{good}} = \frac{C_{Q_h}|p|_k}{C_{V_{00,h}}|\mathbf{u}|_{k+1}}. \tag{3.16}$$

Again, the parameter is different from those obtained for minimizing the $H^1(\Omega)$ error of the velocity. In contrast to (3.8), the parameter (3.16) does not depend on the inverse of ν such that one can expect that for small ν the parameter (3.8) is larger than (3.16).

4 Numerical experiments

Two numerical experiments will be presented in this section. The first one is for an analytic test problem with known solution to support the analysis. In this experiment, the optimal values for γ can be computed and these values will be compared with the predictions from Section 3. The second example is of more practical interest; it is Rayleigh–Bénard convection for silicon oil. Here, an analytic expression for the analytic solution is unknown, but from experiments one can hypothesize that $|p|_2/|\mathbf{u}_3$ is very large, and therefore large grad-div stabilization parameters may significantly improve results. It will be demonstrated that this is indeed the case.

4.1 Optimal stabilization parameters for an analytic test problem

This section will demonstrate that the different regimes for choosing γ_{opt} or γ_{good} given in the previous section can be observed in numerical simulations. For this demonstration, examples with prescribed analytic solutions will be considered. Further steps of the application of the analytic results to more complicated situations will be pointed out in Section 5.

The discretization of the Stokes problem was considered with two choices of conforming inf-sup stable pairs of finite element spaces and with three types of meshes. We consider (2.1) with $\Omega = (0,1)^2$ and with the prescribed velocity solution

$$\mathbf{u} = \begin{pmatrix} \cos(2\pi y) \\ \sin(2\pi x) \end{pmatrix}.$$

Three values for the viscosity will be studied, $\nu \in \{1, 10^{-1}, 10^{-2}\}$, and three different functions that serve as a prescribed pressure solution:

$$p_1 = \sin(2\pi y), \qquad p_2 = \sin(8\pi y), \qquad p_3 = 100\sin(2\pi y).$$

For each of these nine solutions, the forcing $\mathbf{f}$ was computed using the Stokes equation. In all examples, Dirichlet boundary conditions for the velocity were applied. The discrete problem (2.3) was then solved with varying stabilization parameter γ.

The first purpose of these numerical studies was to verify that the analysis-based selections of γ_{opt} or γ_{good}, see (3.7) or (3.8) for the Taylor–Hood finite element, are close to the actual optimal γ, in the sense of minimizing the $H^1(\Omega)$ velocity error. As there are unknown interpolation constants in (3.7) and (3.8), we used the computed optimal γ from coarse meshes to fit the constant(s), and then used it to predict the good values of γ on finer meshes. Secondly, the optimal stabilization parameters were computed also on the basis of minimizing the $L^2(\Omega)$ error of the pressure to show the differences to the velocity case and to illustrate the predictions from Remark 2.

Delaunay triangulations, barycenter refinements of triangular meshes, and Union Jack (criss-cross) meshes were considered. The use of these meshes allows us to study the cases of optimal vs. non-optimal approximation properties of the pointwise divergence-free subspaces of the velocity spaces for the $((P_2)^2, P_1)$ and the $((P_1^{\text{bub}})^2, P_1)$ pairs of finite elements. From [2,18] it is known that the pointwise divergence-free subspace of the $(P_2)^2$ velocity space has optimal approximation properties on a barycenter refinement of a regular mesh. Also, the pointwise divergence-free subspace of the $(P_1^{\text{bub}})^2$ velocity has optimal approximation properties, see [21]. An example of each of the considered mesh types is shown in Figure 1.

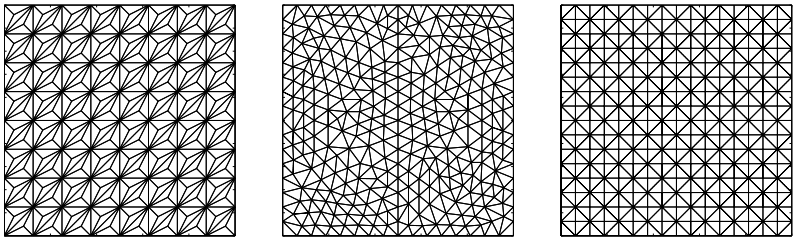

Fig. 1 Barycenter-refined, Delaunay, and Union Jack (criss-cross) meshes (left to right) used in the numerical studies.

4.1.1 $((P_2)^2, P_1)$ *Taylor–Hood element on barycenter-refined meshes*

We consider now $((P_2)^2, P_1)$ Taylor–Hood elements on a barycenter-refined uniform mesh, a case where one knows that the divergence-free subspace of the velocity space has optimal approximation properties. Thus, following the scaling analysis of the previous section, a good choice of γ for this test problem for minimizing the $H^1(\Omega)$ velocity error will satisfy, cf. (3.8),

$$\gamma_{\text{good}} \approx C_0 \frac{1}{2\nu} \frac{|p|_2^2}{|\mathbf{u}|_3^2} = \begin{cases} \dfrac{C_0}{16\nu\pi^2} & \text{for } p_1, \\ \dfrac{4C_0}{\nu\pi^2} & \text{for } p_2, \\ \dfrac{10,000C_0}{16\nu\pi^2} & \text{for } p_3, \end{cases} \tag{4.1}$$

where C_0 is an unknown constant, which is independent of h and γ. Numerical simulations were performed on three meshes, with $h \in \{1/8, 1/16, 1/32\}$ (the $h = 1/8$ mesh is shown in Figure 1 on the left hand side). On this mesh, the actual optimal γ was used, along with (4.1), to approximate C_0 for each of the nine examples. Using these values, choices of γ_{good} based on (4.1) were predicted for the finer meshes. This strategy was applied for all cases of the first numerical experiment.

The results of the numerical studies are presented in Figure 2, for all nine chosen analytic solutions, where the $H^1(\Omega)$ velocity error is plotted against the grad-div stabilization parameter γ. The actual optimal γ is displayed as a downward triangle and the predicted parameter γ_{good} is given as an upward facing triangle. These results indicate that γ_{good} was always a good choice. In addition, the choice γ_{good} leads often to clearly better results than picking $\gamma = 1$ or $\gamma = \mathcal{O}(1)$, e.g., in the bottom right plot, one can see that using the analysis-based selection γ_{good} gives dramatically smaller errors than the solution with $\gamma = 1$, particularly for the case $\nu = 0.01$. Lastly, we note the clear dependence of the optimal γ on ν and its independence of h, both of which are predicted by (4.1).

Results for this test case for the $L^2(\Omega)$ pressure error are shown in Figure 3. One can observe that for larger and more complex pressures, the optimal stabilization parameter increases. This behavior is in agreement with (3.16) since the numerator in this expression becomes larger for complex pressures, although one should keep in mind that (3.16) was derived under the assumption of the maximal possible second term in (3.14). A dependence of the optimal parameter on the mesh width cannot be seen. The optimal γ does not appear to scale with ν significantly, but if there is any dependence, it appears to be inverse from the velocity case. An expectation formulated in Remark 2 was that for small ν the optimal parameter based on minimizing the $H^1(\Omega)$ velocity error should be larger. This expectation is clearly met, in particular for p_2 and p_3, cf. Figs. 2 and 3. It should be noted that the change in the pressure error due to varying γ is relatively small compared with the velocity case.

4.1.2 $((P_2)^2, P_1)$ *Taylor–Hood element on Delaunay-generated triangulations*

Next, we consider the case of $((P_2)^2, P_1)$ Taylor–Hood elements on a Delaunay-generated triangulation, which is a situation where it is not expected that the pointwise divergence-free subspace of the velocity

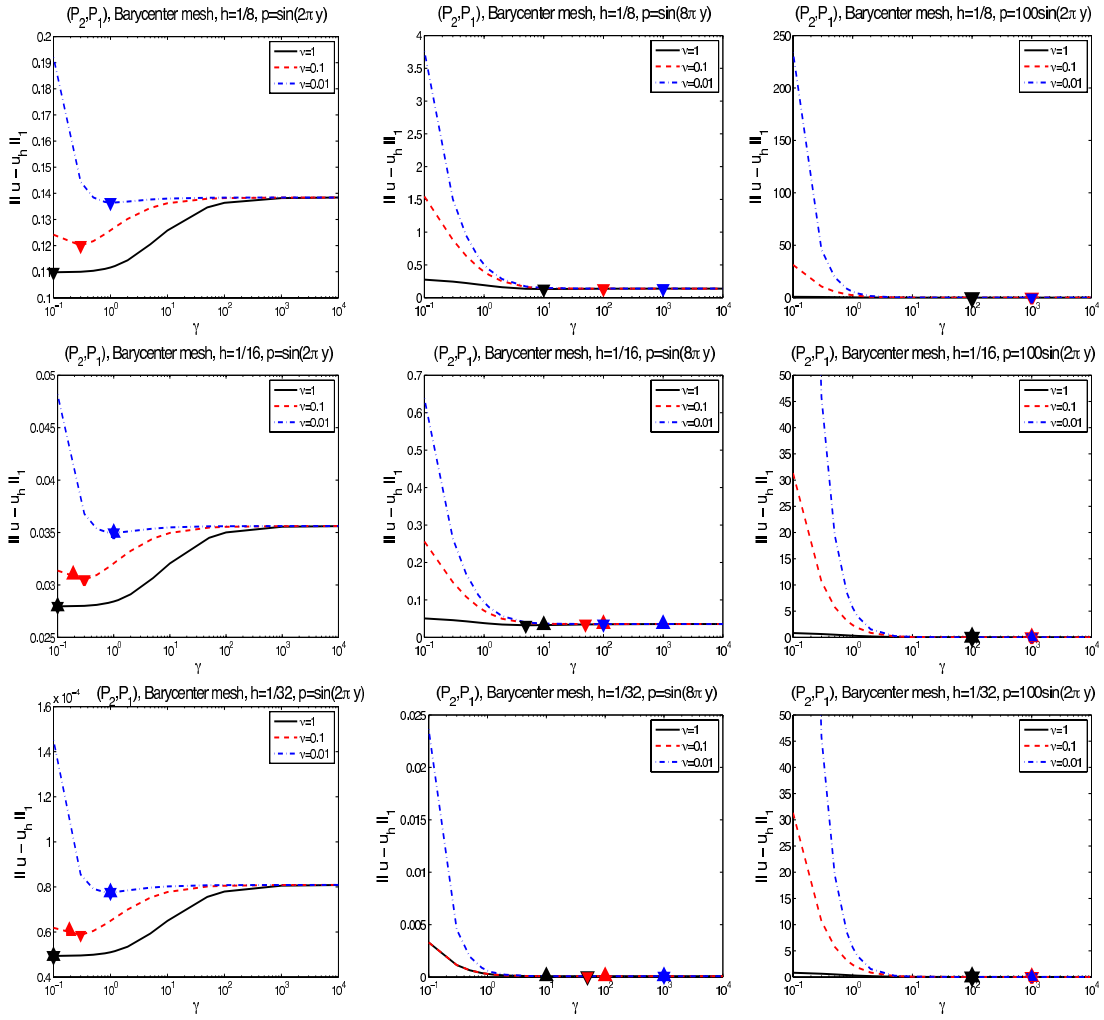

Fig. 2 $H^1(\Omega)$ velocity errors vs. grad-div stabilization parameter γ, for each of the nine chosen Stokes solutions, on successive refinements of barycenter-refined uniform meshes. The actual optimal γ is plotted using a downward triangle and the predicted values γ_{good} are displayed using an upward triangle.

space has optimal approximation properties. Hence, the parameter choice (3.7) should be applied

$$\gamma_{\text{good}} \approx -\nu + \sqrt{\nu^2 + \frac{C_0 |p|_2^2}{|\mathbf{u}|_3^2}} = \begin{cases} -\nu + \sqrt{\nu^2 + \dfrac{C_0}{8\pi^2}} & \text{for } p_1, \\ -\nu + \sqrt{\nu^2 + \dfrac{8C_0}{\pi^2}} & \text{for } p_2, \\ -\nu + \sqrt{\nu^2 + \dfrac{10,000C_0}{8\pi^2}} & \text{for } p_3. \end{cases}$$

This scaling suggests that the γ_{good} will be independent of the mesh width h and it will be essentially independent of ν when ν is small.

The nine test problems were computed on three successively finer Delaunay-generated triangulations with $h \in \{1/8, 1/16, 1/32\}$. The $h = 1/16$ mesh is depicted in Figure 1. Estimates of C_0 were derived in the same way as described above.

The results for these numerical experiments are displayed in Figure 4. They show again that the predicted value γ_{good} is often close to the actual optimal value or that at least the error obtained with γ_{good} is close to the error obtained with the optimal stabilization parameter. Also in this regime, it turns out that picking $\gamma = 1$ or $\gamma = \mathcal{O}(1)$ leads often to considerably worse results than obtained with γ_{good}, particularly for larger pressures and smaller viscosities. Furthermore, the numerical results agree with the theory in the

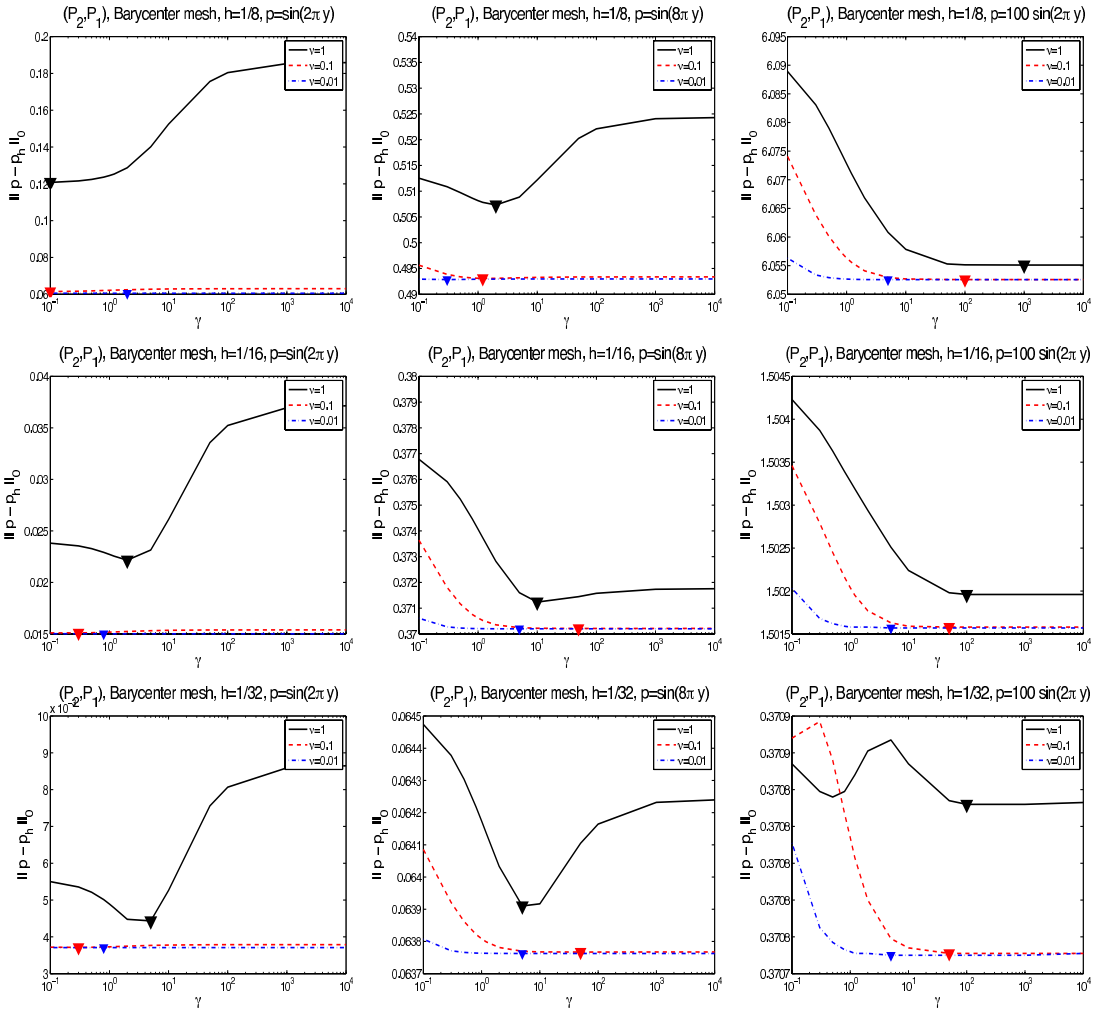

Fig. 3 $L^2(\Omega)$ pressure errors vs. grad-div stabilization parameter γ, for each of the nine Stokes solutions, on three barycenter refined triangulations with $h \in \{1/8, 1/16, 1/32\}$. The actual optimal γ are plotted using a downward triangle.

sense that the a good choice of γ for this case is independent of h and only slightly (if at all) dependent on ν.

Figure 5 presents results with respect to the optimal stabilization parameter obtained by minimizing the $L^2(\Omega)$ error of the pressure. It is again interesting to note that the change in this error due to varying γ is relatively small compared with the velocity case. The optimal stabilization parameters appear to be independent of the mesh width. A clear dependence on ν cannot be observed. Due to Remark 2 it can be expected that the optimal stabilization parameters are smaller than in the velocity case. Comparing the results of Figs. 4 and 5, one finds that this is indeed usually the case.

4.1.3 The Mini element on Union Jack triangulations

Now, the element pair $((P_1^{\text{bub}})^2, P_1)$, the mini element, is considered, which was first studied in [1]. The simulations were performed on meshes of Union Jack type with $h \in \{1/16, 1/32, 1/64\}$, see the right hand side picture in Figure 1 for the coarsest of these meshes. From [21] it is known that on this type of meshes the mini element has the property that the pointwise divergence-free subspace of the velocity space has optimal approximation properties. Arguing the same way as for the Taylor–Hood finite element, the theory derived in the previous section predicts that a good choice of γ should satisfy

$$\gamma_{\text{good}} \approx \frac{C_0 h^2}{2\nu} \frac{|p|_2^2}{|\mathbf{u}|_2^2} = \begin{cases} C_0 h^2 \nu^{-1} & \text{for } p_1, \\ 16 C_0 h^2 \nu^{-1} & \text{for } p_2, \\ 2{,}500 C_0 h^2 \nu^{-1} & \text{for } p_3. \end{cases}$$

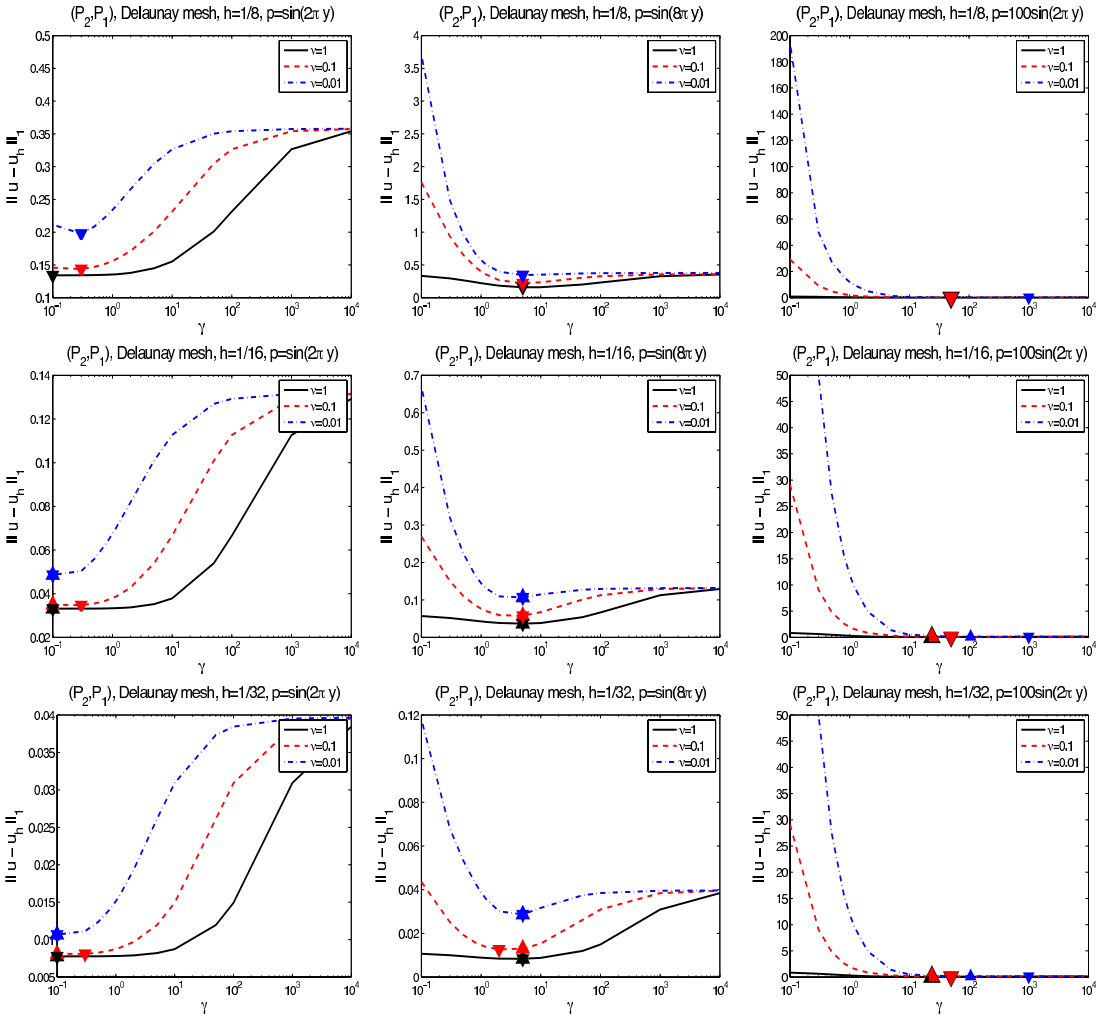

Fig. 4 $H^1(\Omega)$ velocity errors vs. grad-div stabilization parameter γ, for each of the nine Stokes solutions, on three Delaunay-generated triangulations with $h \in \{1/8, 1/16, 1/32\}$. The actual optimal γ are plotted using a downward triangle and the predicted values γ_{good} are displayed using an upward triangle.

Note that there is now a dependence of the parameter on the mesh width, which comes from the equal-order interpolation of the velocity and pressure finite element space. Asymptotically, one has $\gamma_{\text{good}} = \mathcal{O}(h^2)$ and in particular $\gamma_{\text{good}} \to 0$ as $h \to 0$.

Again, the coarsest mesh optimal γ were used to fit the constants C_0. The results of the simulations are presented in Figure 6. They show once more that γ_{good} is always a good choice. For the considered viscosities and pressures, the dependence of the error on γ is much weaker than for the Taylor–Hood finite element. Thus, using γ_{good} instead of $\gamma = 1$ or $\gamma = \mathcal{O}(1)$ leads usually only to somewhat better results. The differences might increase if different examples are considered. The dependence of the optimal γ on h and ν, that is predicted by the analysis, can be clearly observed.

4.1.4 The mini element on Delaunay-generated triangulations

Finally, the mini element on Delaunay-generated triangulations will be considered, where one does not expect the divergence-free subspace of the velocity space to have optimal approximation properties. Hence, the optimal stabilization parameter should be derived with the same arguments that were used to get (3.7). Applying these arguments, one finds that the optimal stability parameter should satisfy

$$\gamma_{\text{good}}^2 + 2\nu\gamma_{\text{good}} - C_0 h^2 \frac{|p|_2^2}{|\mathrm{u}|_2^2} \approx 0.$$

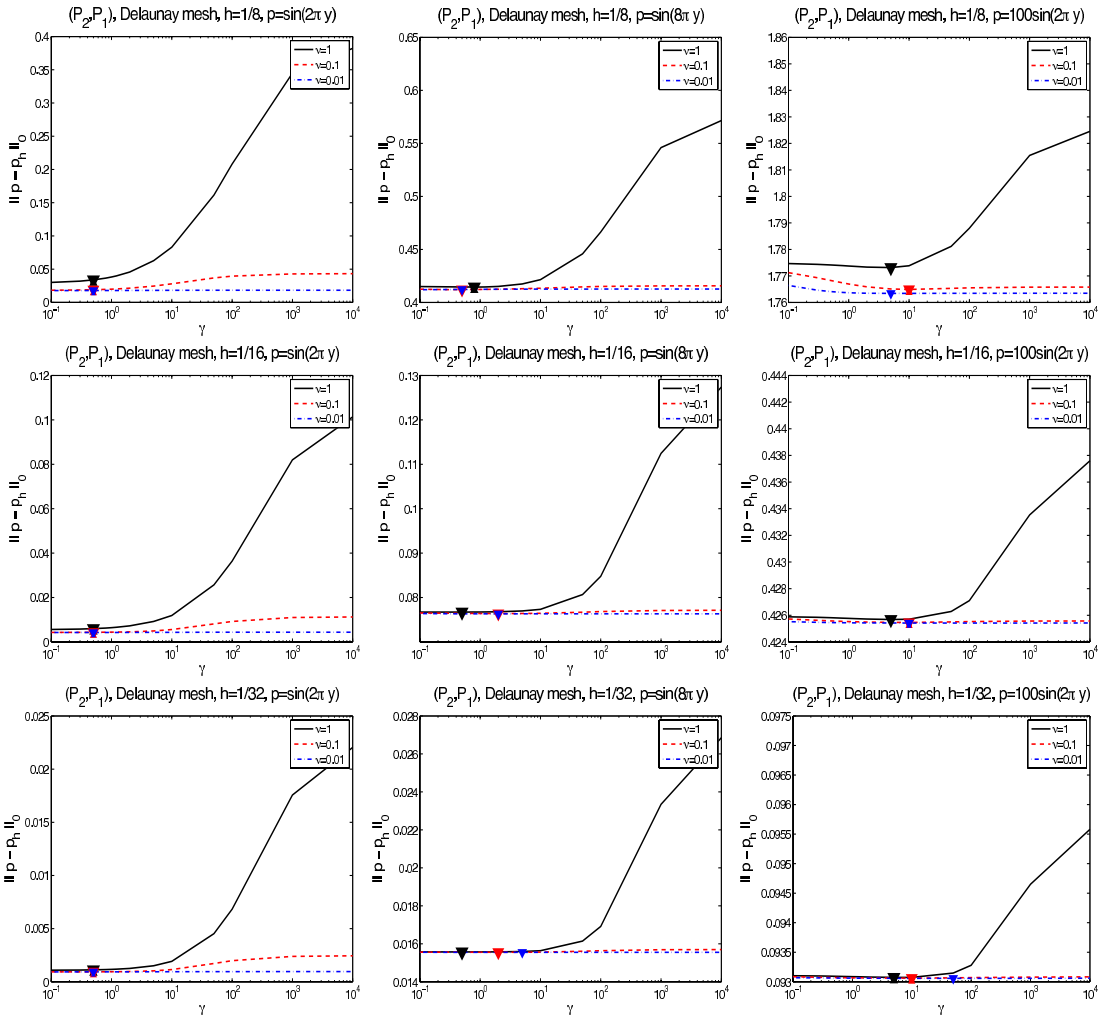

Fig. 5 $L^2(\Omega)$ pressure errors vs. grad-div stabilization parameter γ, for each of the nine Stokes solutions, on three Delaunay-generated triangulations with $h \in \{1/8, 1/16, 1/32\}$. The actual optimal γ are plotted using a downward triangle.

It follows that

$$\gamma_{\text{good}} \approx -\nu + \sqrt{\nu^2 + C_0 h^2 \frac{|p|_2^2}{|\mathbf{u}|_2^2}} = \begin{cases} -\nu + \sqrt{\nu^2 + \dfrac{C_0 h^2}{2\pi^2}} & \text{for } p_1, \\ -\nu + \sqrt{\nu^2 + \dfrac{32 C_0 h^2}{\pi^2}} & \text{for } p_2, \\ -\nu + \sqrt{\nu^2 + \dfrac{5{,}000 C_0 h^2}{\pi^2}} & \text{for } p_3. \end{cases}$$

The results of the numerical studies for this setup are presented in Figure 7. Again, one can observe that the analysis-based parameter γ_{good} was always a good choice. In particular, the results were in general better than generically picking $\gamma = 1$. The dependence on h, although weaker than in the case of Union Jack meshes, can be observed. Also, as predicted, there does not appear to be a significant dependence on ν.

4.2 Rayleigh–Bénard convection for silicon oil

The second test problem we consider is the differentially heated cavity on the unit square with Rayleigh number $\text{Ra} = 10^6$, Prandtl number $\text{Pr} = \infty$ (corresponding to silicon oil), with no slip boundary conditions for the velocity, and mixed Dirichlet/Neumann conditions for the temperature, see Figure 8. Since $\text{Pr} = \infty$,

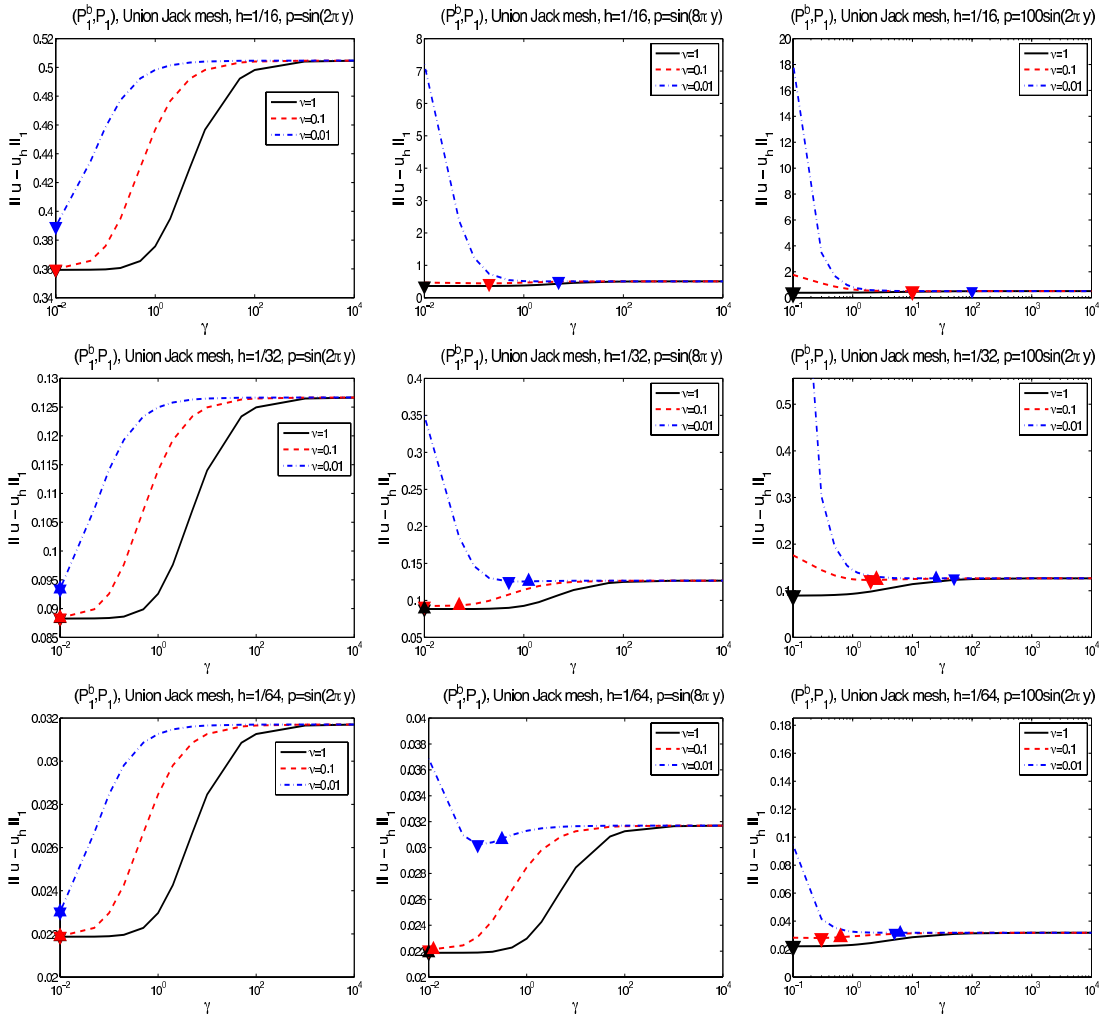

Fig. 6 $H^1(\Omega)$ velocity errors vs. grad-div stabilization parameter γ, for each of the nine chosen Stokes solutions, using the mini element on Union Jack triangulations with $h \in \{1/16, 1/32, 1/64\}$. The actual optimal γ is plotted using a downward triangle and the predicted values γ_{good} are displayed using an upward triangle.

the system of equations that governs this flow is given by

$$\begin{aligned} -\Delta \mathbf{u} + \nabla p &= (0, \mathrm{Ra}\, T)^{\mathrm{T}} && \text{in } \Omega, \\ \nabla \cdot \mathbf{u} &= 0 && \text{in } \Omega, \\ -\Delta T + \mathbf{u} \cdot \nabla T &= 0 && \text{in } \Omega. \end{aligned}$$

Although this system is nonlinear because of the energy equation, the momentum equation is a Stokes equation. Thus, the theory developed in this paper is applicable.

This system was implemented with a standard finite element approach, see, e.g., [8], using $(V_h, Q_h) = ((P_2)^2, P_1)$ Taylor–Hood elements to approximate velocity and pressure, respectively, and $X_h = P_2$ to approximate temperature. The finite element formulation for a specified Ra takes the form: Find $(\mathbf{u}_h, p_h, T_h - T_{d,h}) \in V_h \times Q_h \times X_h$ such that for all $(\mathbf{v}_h, q_h, s_h) \in V_h \times Q_h \times X_h$

$$\begin{aligned} \nu(\nabla \mathbf{u}_h, \nabla \mathbf{v}_h) + \gamma(\nabla \cdot \mathbf{u}_h, \nabla \cdot \mathbf{v}_h) - (\nabla \cdot \mathbf{v}_h, p_h) &= ((0, Ra\, T_h)^{\mathrm{T}}, \mathbf{v}_h), \\ (\nabla \cdot \mathbf{u}_h, q_h) &= 0, \\ (\nabla T_h, \nabla s_h) + (\mathbf{u} \cdot \nabla T_h, s_h) &= 0, \end{aligned} \tag{4.2}$$

where $T_{d,h}$ is an extension of the Dirichlet data to the finite element space with inhomogeneous Dirichlet boundary conditions. The nonlinearity of (4.2) is resolved using Newton's method, to a relative difference of 10^{-10} in successive iterates. We also found it necessary to use a continuation method in Ra to get

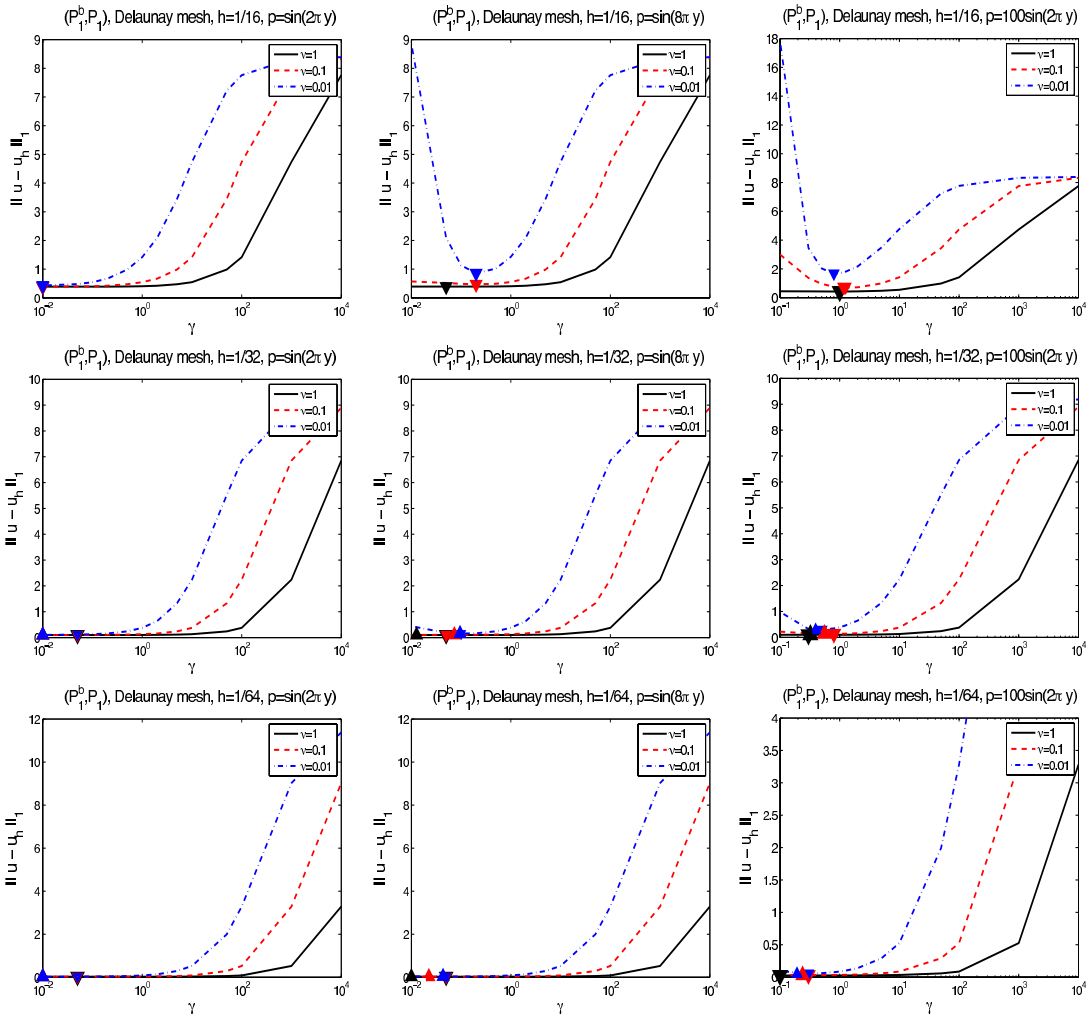

Fig. 7 $H^1(\Omega)$ velocity errors vs. grad-div stabilization parameter γ, for each of the nine Stokes solutions, using the mini element on Delaunay-generated triangulations with $h \in \{1/16, 1/32, 1/64\}$. The actual optimal γ is plotted using a downward triangle and the predicted values γ_{good} are displayed using an upward triangle.

convergence with $\text{Ra} = 10^6$ (via $\text{Ra} \in \{10^4, 10^5, 10^6\}$), and each Newton iteration typically took 4 or 5 iterations to converge. Plots of the resolved solution's velocity streamlines, pressure contours, speed contours, and temperature contours are shown in Figure 9. Observe that the size of the pressure p_h is on the order of 10^5, while the speed $|\mathbf{u}_h|^2$ is on the order of 10^2, and hence the size of the velocity is on the order 10^1. Thus, the ratio of the size of the pressure to the size of the velocity is very large, and from the contour plots one can expect $|p|_2/|\mathbf{u}|_3$ to be large as well. Considering this problem on a coarse mesh, a larger velocity error (compared with the reference solution) can be expected that is dominated by the contribution from the pressure. The analysis presented in this paper suggests that this contribution can be reduced by increasing the grad-div stabilization parameter γ, thereby reducing the overall error, and finally leading to significantly improved solutions for the velocity.

We computed solutions to (4.2), using $((P_2)^2, P_1, P_2)$ elements for velocity-pressure-temperature, on the mesh shown in Figure 10 that provided 3,679 total degrees of freedom, with varying grad-div stabilization parameter γ. Solutions are shown in Figure 11, as velocity streamlines and temperature contours. Comparing with the resolved solution in Figure 9, the temperature contours agree for all solutions except when $\gamma = 0$, but the velocity streamlines are correct only for the $\gamma = 1,000$ and $\gamma = 10,000$ simulations. Hence, one observes an increase in accuracy from the use of large grad-div stabilization parameters, as expected. A similar observation was reported in [7] for the case $\text{Pr} = 1$.

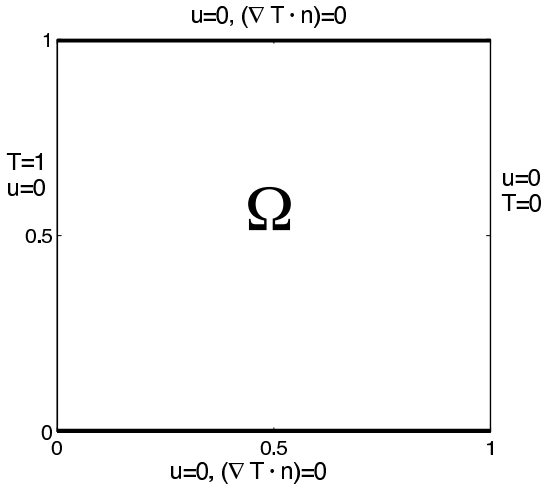

Fig. 8 The domain and boundary conditions for the natural convection problem.

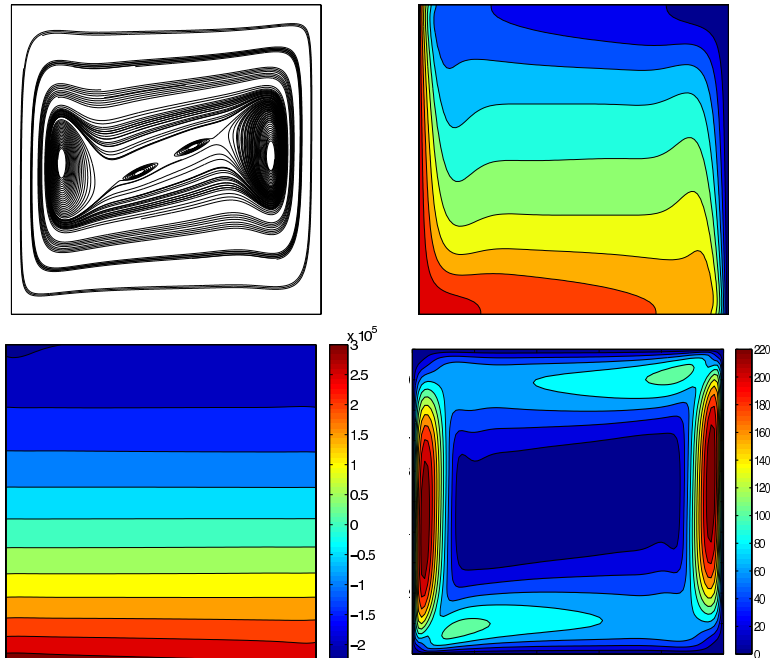

Fig. 9 The velocity streamlines (top left), temperature contours (top right), pressure contours (bottom left), and speed contours (bottom right) of the resolved solution to the differentially heated cavity.

5 Conclusions and outlook

A re-investigation of the question of optimal grad-div stabilization parameters in finite element methods for the Stokes equations was presented that clarified that one has to distinguish several situations for designing such a parameter for conforming inf-sup stable pairs of finite element spaces, depending on whether the $H^1(\Omega)$ error of the velocity or the $L^2(\Omega)$ error of the pressure is of interest. It was demonstrated that the question of the existence of a divergence-free subspace with optimal approximation properties is crucial. Consequently, the optimal parameter choice does not even have the same expression within classes of finite element spaces, e.g. within the class of Taylor–Hood finite elements, as it depends on the concrete space itself, i.e. on the properties of the grid and the element choice together. In addition, the regularity of the solution also plays a role for the optimal stabilization parameter. Based on estimate (3.1), one can derive parameters for solutions with reduced smoothness by applying interpolation estimates to spaces with appropriate regularity.

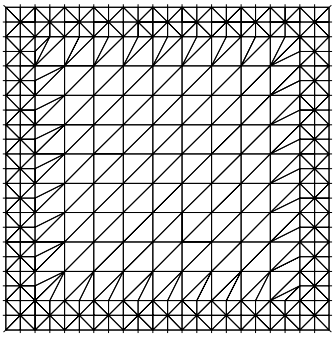

Fig. 10 The mesh used for the differentially heated cavity problem.

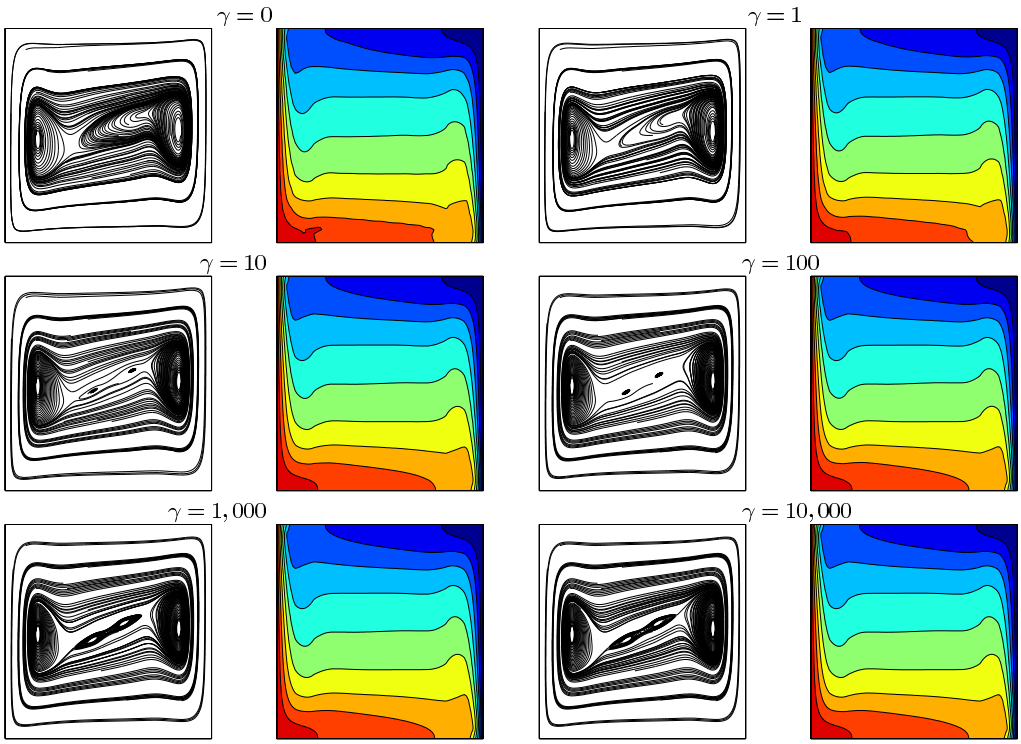

Fig. 11 Differentially heated cavity problem: velocity streamlines and temperature contours of solutions with varying γ.

The present paper gave an analytic support for the observation from [8] that the use of large stabilization parameters is appropriate in certain situations. Numerical studies were presented that support the analytic results. Moreover, and particularly important for applications, an enormous error reduction (in the $H^1(\Omega)$ error of the velocity) could be observed in certain cases by using parameters predicted from the present analysis instead of parameters of $\mathcal{O}(1)$, as they were proposed in the literature (based on error estimates for other norms). Also in a more complex flow problem, the choice of large stabilization parameters resulted in considerable improvements of the computed velocity field.

Extending the analytic considerations to more complex equations or systems from Computational Fluid Dynamics will result in more terms on the right hand side of the error estimates. Hence, it will become more complicated to derive information about a good value of the stabilization parameters. This issue will be studied in future work. Also from the practical point of view, a number of issues need to be addressed. How to determine whether the divergence-free subspace of the finite element velocity has optimal approximation properties? How to estimate parameters of form (3.7) or (3.8) efficiently without knowledge of the analytic solution? We think that none of these questions can be answered easily. Altogether, there are a number of topics for further research on the grad-div stabilization.

References

1. D. Arnold, F. Brezzi, and M. Fortin. A stable finite element for the Stokes equations. Calcolo, 21(4):337–344, 1984.
2. D. Arnold and J. Qin. Quadratic velocity/linear pressure Stokes elements. In R. Vichnevetsky, D. Knight, and G. Richter, editors, Advances in Computer Methods for Partial Differential Equations VII, pages 28–34. IMACS, 1992.
3. M. Braack, E. Burman, V. John, and G. Lube. Stabilized finite element methods for the generalized Oseen problem. Comput. Methods Appl. Mech. Engrg., 196(4-6):853–866, 2007.
4. S. Brenner and L. R. Scott. The Mathematical Theory of Finite Element Methods. Springer-Verlag, 1994.
5. Y. Bychenkov and E.V. Chizonkov. Optimization of one three-parameter method of solving an algebraic system of Stokes type. Russ. J. Numer. Anal. Math. Model, 14:429–440, 1999.
6. M. Case, V. Ervin, A. Linke, and L. Rebholz. A connection between Scott-Vogelius elements and grad-div stabilization. SIAM Journal on Numerical Analysis, 49(4):1461–1481, 2011.
7. O. Dorok, W. Grambow, and L. Tobiska. Aspects of finite element discretizations for solving the Boussinesq approximation of the Navier-Stokes Equations. Notes on Numerical Fluid Mechanics: Numerical Methods for the Navier-Stokes Equations. Proceedings of the International Workshop held at Heidelberg, October 1993, ed. by F.-K. Hebeker, R. Rannacher and G. Wittum, 47:50–61, 1994.
8. K. Galvin, A. Linke, L. Rebholz, and N. Wilson. Stabilizing poor mass conservation in incompressible flow problems with large irrotational forcing and application to thermal convection. Computer Methods in Applied Mechanics and Engineering, 237:166–176, 2012.
9. R. Glowinski and P. Le Tallec. Augmented Lagrangian and operator splitting methods in nonlinear mechanics. SIAM, Studies in Applied Mathematics, Philadelphia, 1989.
10. T. Heister and G. Rapin. Efficient augmented Lagrangian-type preconditioner for the Oseen problem using grad-div stabilization. Int. J. Numer. Meth. Fluids, 71:118–134, 2013.
11. V. John and A. Kindl. Numerical studies of finite element variational multiscale methods for turbulent flow simulations. Comput. Methods Appl. Mech. Engrg., 199(13-16):841–852, 2010.
12. W. Layton. An Introduction to the Numerical Analysis of Viscous Incompressible Flows. SIAM, 2008.
13. W. Layton, C. Manica, M. Neda, M. A. Olshanskii, and L. Rebholz. On the accuracy of the rotation form in simulations of the Navier-Stokes equations. Journal of Computational Physics, 228(9):3433–3447, 2009.
14. C. Manica, M. Neda, M. A. Olshanskii, and L. Rebholz. Enabling accuracy of Navier-Stokes-alpha through deconvolution and enhanced stability. M2AN: Mathematical Modelling and Numerical Analysis, 45:277–308, 2011.
15. M. A. Olshanskii. A low order Galerkin finite element method for the Navier-Stokes equations of steady incompressible flow: a stabilization issue and iterative methods. Comput. Meth. Appl. Mech. Eng., 191:55155536, 2002.
16. M. A. Olshanskii, G. Lube, T. Heister, and J. Löwe. Grad-div stabilization and subgrid pressure models for the incompressible Navier-Stokes equations. Comput. Methods Appl. Mech. Engrg., 198(49-52):3975–3988, 2009.
17. M. A. Olshanskii and A. Reusken. Grad-Div stabilization for the Stokes equations. Math. Comp., 73:1699–1718, 2004.
18. J. Qin. On the convergence of some low order mixed finite elements for incompressible fluids. PhD thesis, Pennsylvania State University, 1994.
19. H.-G. Roos, M. Stynes, and L. Tobiska. Robust numerical methods for singularly perturbed differential equations, volume 24 of Springer Series in Computational Mathematics. Springer, Berlin, 2nd edition, 2008.
20. L. Tobiska and R. Verfürth. Analysis of a streamline diffusion finite element method for the Stokes and Navier-Stokes equations. SIAM J. Numer. Anal., 33:107–127, 1996.
21. S. Zhang. Bases for C0-P1 divergence-free elements and for C1-P2 finite elements on union jack grids. Submitted, 2012.